

**Cigré Prototype Installation Test for Gas-Insulated DC Systems –
Testing a Gas-Insulated DC Transmission Line (DC-GIL) for ± 550 kV and 5000 A under Real
Service Conditions**

**M. HALLAS¹, V. HINRICHSSEN¹, C. NEUMANN¹, M. TENZER², B. HAUSMANN², D. GROSS³,
T. NEIDHART⁴, M. LERCH⁴, D. WIESINGER⁴**

¹ Technische Universität Darmstadt, High Voltage Laboratories

² Siemens Gas and Power, Erlangen

³ Power Diagnostix, Aachen

**⁴ Ostbayerische Technische Hochschule Regensburg, Geotechnics
Germany^{1, 2, 3, 4}**

SUMMARY

More and more generation facilities are installed far away from the load centers. Thus, long distance transmission is demanded, and with this regard DC transmission systems are of special interest. Transmission by overhead lines is a well-proven technology, but due to environmental concern and political decisions underground transmission systems are often requested. Besides DC cables, DC GIL are an interesting option. They enable transmitting high power by only one system in a small corridor only a few meters wide. GIL can be laid in a tunnel or directly buried in the soil. Meanwhile a lot of service experience has been collected with AC GIL technology, but no service experience is yet available with DC GIL. To close this knowledge gap and to investigate the long-term performance, a ± 550 kV DC GIL prototype with a current carrying capacity of 5000 A is currently investigated in a HVDC test facility, both in directly buried and in above-ground installation. The test procedure follows the recommendations for long-term testing of gas-insulated systems, currently under preparation by Cigré JWG D1/B3.57. This report describes the test sample arrangements, the high-voltage and high current test equipment and the commissioning procedure for the DC GIL. It illustrates the UHF PD monitoring system installed and the method to identify possible PD defects. The investigated DC GIL is subdivided into two parts: While an above-ground installation is simultaneously stressed by voltage and DC current, a directly buried part of the DC GIL is stressed with DC current only in order to investigate soil mechanics, the temperature distribution in the GIL and in the soil as well as the performance of the backfill material. The report also presents first results gained on the directly buried arrangement for studying the soil mechanics.

KEYWORDS

DC GIL, prototype installation test, UHF DC PD measurement, UHF monitoring, DC current injection, superimposed voltage testing, soil mechanics, soil temperature, soil-structure-interaction

1. Introduction

The technology of gas-insulated transmission lines (GIL) was introduced in the 1970s for AC current transmission [1]. The principle design of a DC GIL (Figure 1, (a)) is similar to the AC GIL design, consisting of two coaxial aluminum tubes: the inner conductor and the outer enclosure. The inner conductor is supported and centered by tripod cast-resin insulators. The endlessly welded aluminum enclosure ensures a solid mechanical and electrical encapsulation of the system. Particle traps are provided to capture free moving particles, which cannot totally be avoided during assembly and installation. At the construction site, pre-assembled GIL structures in lengths of 10...20 m are welded together to form the final GIL transmission line. After several hundred meters each, disc insulators are installed to compensate the thermal expansion of the inner conductor by a sliding contact and to separate the gas compartments if required. Since the 2000s, GIL with a gas mixture of nitrogen (N_2) and SF_6 are available. Major advantages of the GIL technology are high transmission power, low losses, low capacitance, high safety in case of internal arcs and non-flammable technology, which does not contribute to fire load. The latter aspects are of high importance especially for tunnel installations of GIL (Figure 1, (b)).

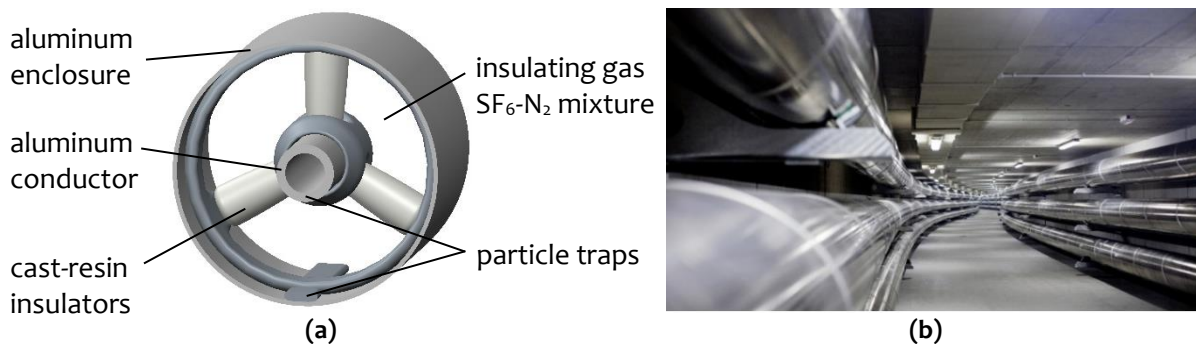


Figure 1: DC-GIL design (a) and application example (two AC systems) in a tunnel installation (b) [2]

Several high-voltage direct current (HVDC) transmission links are currently being planned worldwide, mainly in order to transmit renewable power over large distances at low losses. The investigated DC GIL, directly buried or installed in a tunnel, is able to transmit 5 GW electrical power at a corridor width of approximately 6 m, which is considerably smaller and less space consuming than comparable cable or overhead line installations [3]. To meet the future demand of HVDC underground transmission systems, a prototype of a DC GIL for up to ± 550 kV DC voltage has been developed based on the AC GIL technology [4]. Its rated current is 5000 A, providing reserves for future converters with higher currents, overload capability or lower losses and heating under partial load. The major new developments for the DC GIL (in comparison with AC GIL) are adapted insulators and novel particle traps. The DC GIL insulators are made of an adapted epoxy cast resin and an adapted geometry in a way that they are suitable both for AC and DC voltage stress. The DC GIL particle traps consider the particular particle movement phenomena at positive and negative polarity of direct voltage at the enclosure and the conductor [5], [6].

To investigate the long-term performance, the ± 550 kV DC GIL prototype is currently examined in a HVDC test facility, both in directly buried and in above-ground installation. The tested DC GIL is subdivided into two parts: While an above-ground installation ("Installation A") is simultaneously stressed by voltage and DC current, a directly buried part of the DC GIL ("Installation B") is stressed with DC current only in order to determine soil mechanics, the temperature distribution in the GIL and in the soil as well as the performance of the backfill material. This report describes the test sample arrangements, the high-voltage and high current test equipment and the commissioning procedure for the DC GIL. It illustrates the UHF PD monitoring system installed and the method to identify possible PD defects, and it also presents first results gained on the directly buried arrangement for studying the soil mechanics.

2. Cigré Prototype Installation Test

Prior to any installation in the grid, transmission system operators usually request proofs of a reliable long-term performance under real service conditions, especially in case of larger investments. DC GIL must be able to withstand high overvoltage stress superimposed to the DC voltage at some hundred insulators and particle movement effects after on-site installation. These phenomena are difficult to test adequately on small test samples as it is usually done during type tests in the laboratory. Furthermore, no service experience is available with the new DC GIL design, which makes it essential to gain first service experience in long-term tests. DC cables are tested and qualified by one year “prequalification tests”. DC GIL needs a similar evidence for long-term reliability. In conclusion, first representative DC GIL long-term tests are required to demonstrate the technology readiness level. Cigré JWG D1/B3.57 proposes a “prototype installation test” for gas-insulated DC systems in this context to cover this lack of experience [7]. The test sequence of the Cigré prototype installation test is divided into three parts: pre-test, long-term test and condition check after the test. One of the current Cigré JWG D1/B3.57 proposals for the long-term test sequence is shown in Table 1.

Table 1: One of current Cigré JWG D1/B3.57 proposals for the prototype installation long-term test sequence. HL = high current load; ZL = zero load; U_T = continuous DC test voltage; LI = lightning impulse voltage; SI = switching impulse voltage

		HL 1				ZL				HL 2			
		+		-		+		-		+		-	
		HL	LI	HL	SI	ZL	LI	ZL	SI	HL	LI	HL	SI
Days		30	LI	30	SI	30	LI	30	SI	30	LI	30	SI
Voltage		U_T	U_T	U_T	U_T	U_T	U_T	U_T	U_T	U_T	U_T	U_T	U_T
		U_T	U_T	U_T	U_T	U_T	U_T	U_T	U_T	U_T	U_T	U_T	U_T

This test sequence is applied to the dielectric setup (“Installation A”) of the overall arrangement (chapter 3). The pre-test shall proof the integrity of test object before the long-term operation. The contact system is tested by thermo-mechanical pre-stress, the proper dielectric conditions are verified by superimposed impulse voltage tests and by partial discharge (PD) measurements.

The performance of the insulating system at maximum continuous DC voltage and rated current stress (“HL” in Table 1) is the biggest challenge in HVDC design. After energizing, the electric field distribution changes from capacitive to resistive, and volume and surface charges in the insulation material and at the gas-solid interfaces are generated [7]. The most critical electrical stresses at the DC insulators will occur during the highest temperature gradients across the insulators [9]. Therefore, two “HL” cycles with a test voltage of $U_T = 1.2 U_r$ (U_r =rated voltage) are proposed. As the long-term test is to be considered as an accelerated procedure, the increased voltage U_T is chosen. Furthermore, one zero load (“ZL”) cycle shall be performed to simulate low or zero load service conditions. This is important, as the electric field distribution in the system is affected by temperature gradients, which depend on the actual load condition. The total testing time is 360 days. Each DC voltage polarity is tested for 30 days, which is a compromise and considered reasonable to activate volume and surface charges. Each cycle ends with superimposed impulse voltage tests with lightning or switching voltage of all polarity combinations. This verifies the overvoltage performance of the equipment. The test procedure A of IEC 60060-1 is used (3 impulses – no flashovers), because a flashover across the insulator surface would affect the initial field distribution. To ensure that the overvoltage stress is in accordance with the overvoltage stress in service, it is recommended to apply 80 % of the rated LI and SI voltage level corresponding to the coordination withstand voltage according to the insulation coordination procedure for gas-insulated systems [7].

Lightning impulse voltage testing of large test arrangements, like a DC GIL, will cause travelling wave effects, resulting in unreasonable testing [8]. The propagation time for a 100 m GIL is in the

range of $0.3 \mu\text{s}$ (propagation speed $v \approx c_0 \approx 300 \text{ m}/\mu\text{s}$), which is in the range of the rise time of a standard LI voltage with a front time of $1.2 \mu\text{s}$. To avoid these travelling wave effects, larger front times of the lightning impulse voltage have to be applied. In practice, these problems can also be solved by using oscillating impulse voltages (OLI/OSI - according to IEC 60060-3) with a corresponding frequency. OLI/OSI advantageously results in more compact generators as conventional LI/SI types, why this type of voltage is used for on-site testing of gas-insulated systems. According Cigré JWG D1/B3.57, OLI and OSI voltages can be used to perform the superimposed voltage tests during the prototype installation test. After the long-term test, a PD measurement under AC or DC is carried out to prove the dielectric integrity of the equipment.

3. Dielectric test arrangement (“Installation A”)

The “prototype installation test” proposed by Cigré JWG D1/B3.57 (Clause 2) is implemented by means of the dielectric test arrangement “Installation A”. In advance to this test, numerous appropriate tests on the DC GIL modules were carried out in the laboratory [4]. “Installation A” (Figure 2) is constructed of eight DC GIL straight modules (2) and two 45° DC GIL angle modules (3). The total current loop is approximately 100 m long, installed above-ground and mostly outdoor. This enables easy access to the modules and further represents a critical practical arrangement for the insulation system. At low temperatures, the temperature gradient from the current carrying inner conductor and the naturally cooled enclosure will be most critical. At high ambient temperature and sun irradiation, the temperature gradient may even change its direction at “ZL” cycles. In order to generate even higher temperature gradients, inner GIL conductors of lower wall thickness, rated for approximately 3150 A DC, are installed. The transition time from a capacitive to a resistive field for estimated HL-temperatures will be in the range of approx. 3 to 7 days for the DC GIL insulators under considerations. Thereby, realistic critical stresses of the DC insulation system will be tested adequately by the 30 days test sequence. At least five DC GIL insulators of every type (gas-tight and support insulators) are included in the test setup (2). Approximately 35 insulators plus several insulating rods in switching devices are installed in the overall test assembly.

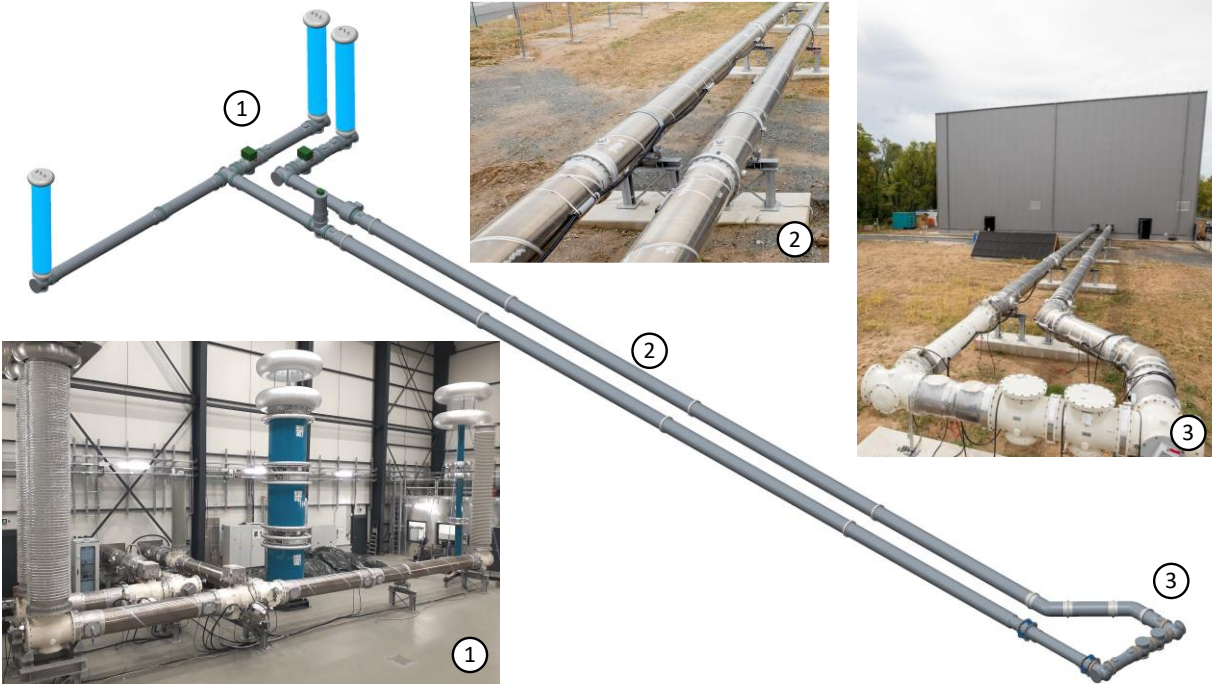


Figure 2: HVDC hall with dielectric indoor (1) and outdoor (2+3) test assembly (“Installation A” – 100 m)

The test equipment for feeding the DC GIL with current and voltage is installed in a high voltage hall (1) (and Figure 2 (3) and Clause 3.1). The current loop of the test setup is connected by

± 550 kV DC GIS modules and a lateral compensation module (3). The test arrangement is equipped with UHF partial discharge (PD) sensors, optical PD and light sensors and temperature measurement systems for monitoring of the conductor and the enclosure temperatures (pyrometers and PT100 sensors), besides the mandatory monitoring systems such as gas density meters.

3.1. Current and voltage testing

The overall “Installation A” test assembly and the basic test circuit is shown in Figure 3. The DC GIL consists of the inner conductor (7), the enclosure (5), the solid insulation (8) and the gas insulation (9). For connecting the different test generators (DC voltage (12), impulse voltage (13), DC current (1)), different ± 550 kV DC GIS modules [9] are used inside the high-voltage hall. Two gas-to-air bushings (3) are installed in parallel for feeding the DC current of up to 5000 A at a high-voltage potential of 660 kV DC. Often DC test assemblies are fed with AC current in order to heat the inner conductor. AC current injection can easily be realized with reversely operated AC current transformers [10]. But AC current feeding has some technical limits. Considering the 100 m GIL test loop, an inductance of approximately 50 μH would have to be fed with up to 5000 A at 50 Hz. This would result in a total reactive power demand of ≈ 400 kVar. Reactive power compensation is possible, but has practical challenges. DC current heating requires less than 30 kW active power to heat the inner conductor by a current of 5000 A DC. DC current heating is thus, on the one hand, a very efficient option to feed the 100 m DC-GIL loop. On the other hand, the DC current operation is equal to the later DC GIL operation in the grid, which ensures thermal stresses equal to practice. To fulfil the task of DC current injection, the power transmission path (2) has to insulate the high DC voltage while simultaneously feeding the current into the DC GIL. The technical solution is explained in Clause 3.1.1.

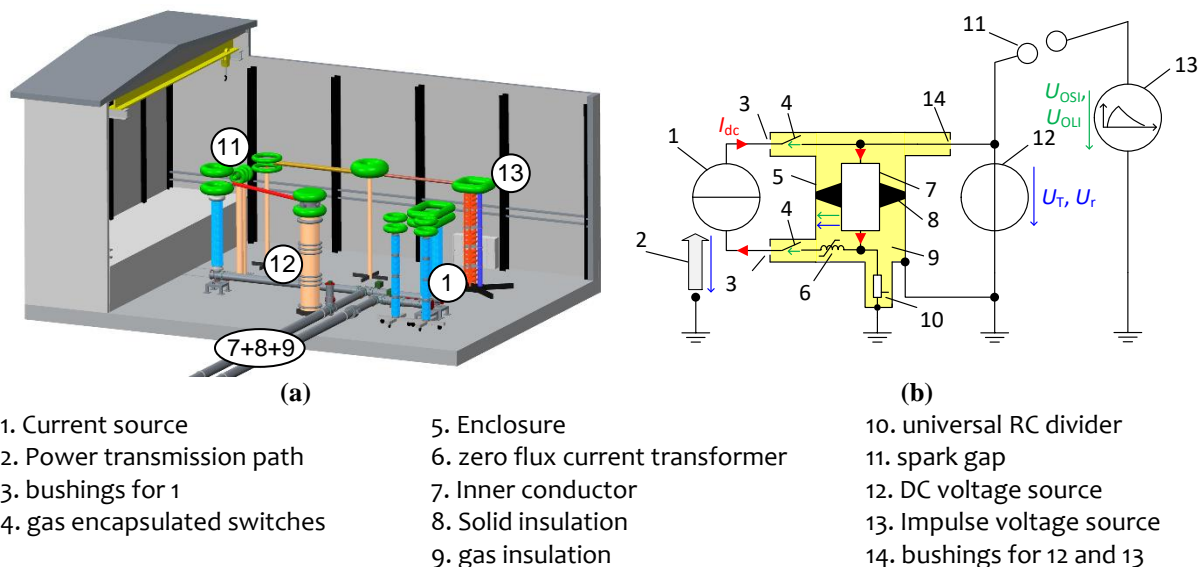


Figure 3: High-voltage test setting for the Cigré Prototype Installation Test; (a) high-voltage/high current test setup; (b) single line diagram of the overall test setup

Behind the two bushings for DC current injection (3), automated disconnectors and earthing switches (4) are installed for disconnecting and earthing the current generator and protecting it from damage during impulse voltage tests. The third, single bushing (14) is intended for applying the DC voltage (12) and the superimposed impulse voltages U_{OLI} , U_{OSI} (13). The superposition is achieved by the use of a spark gap (11). Further details are explained in section 3.1.2. An instrument current transformer according to the zero flux principle (6) measures the DC test current [11]. An

encapsulated universal R-C voltage divider (10) measures the DC and transient voltages directly at the test object.

3.1.1 DC current injection on high voltage potential

Various solutions are possible to inject high DC current on high voltage potential [10]. The capacitive current transmission is an efficient concept to achieve high voltage and current ratings by stacking several components [10]. The basic circuit is shown in Figure 4 [12]. Capacitors are applied to insulate the high DC voltage U_{DC} and to simultaneously transmit

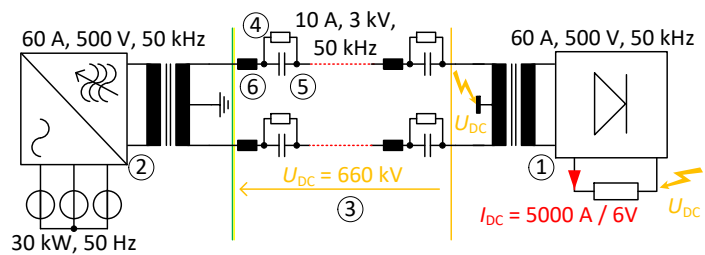


Figure 4: Current injection I_{DC} on high DC voltage potential U_{DC} by capacitive current transmission [12]

power by a high frequency current, making use of the low impedance of the capacitors at high frequencies. An AC/AC converter (2) generates a one-phase current in the 50 kHz frequency range. This current is transferred from earth to the high voltage potential through the capacitive transmission path (3). It consists of several capacitors (5) and compensation coils (6) in series. The overall circuit operates in resonance, thus minimizing reactive power flow through the transmission path. To achieve this, the AC/AC converter (2) is self-adjusting to resonant frequency. On the high voltage potential, the high frequency current feeds a rectifier (1), which generates a test current of up to 5000 A DC. First operation experiences with prototypes and individual components of the generator have proven good performance of the concept [12].

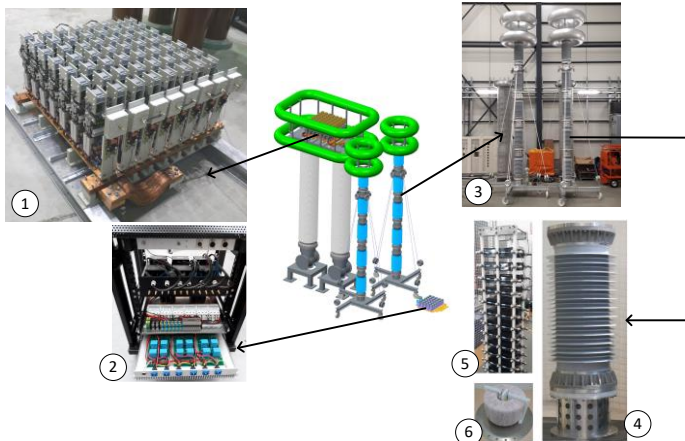


Figure 5: DC current injection source and its components [12]

The total assembly is shown in Figure 5. The AC/AC converter feeding unit is installed on earth potential (2). A modular rectangular converter is used, with MOSFET converter modules operating in parallel. The individual converter module outputs are summed up to the overall output voltage of 0.5 kV via serial connection of switching transformers in each module. The transmission path (3) transfers a current of $I = 10 \text{ A}$ at $U = 3 \text{ kV}$ and $f \approx 50 \text{ kHz}$. Numerous 2.5 kV capacitors (5) are stacked to achieve the desired voltage rating of 660 kV. The compensation coils (6) are toroidal air coils wound with litz wire. This design has no high frequency stray field and is still able to manage the thermal stresses due to high frequency. The rectifier (1) is built modularly with several parallel M2 diode rectifier modules. The modules are connected via switching transformers with serial connection of the primary and parallel connection of the secondary windings. Thus, the power signal is converted from 60 A / 0.5 kV to 5000 A / 6 V at 50 kHz.

3.1.2 Superimposed voltage testing

Superimposed (SIMP) impulse voltages can be coupled to the DC voltage circuit by two different ways: spark gaps or coupling capacitors [13]. In this project, a decision was made to use spark gaps. Spark gaps are reliable, robust, easy to realize and cost efficient. Furthermore, the impulse voltage generator can be dimensioned smaller to achieve the same voltage ratings. For example, a spark gap setup needs about $\pm 1550 \text{ kV}$ generator output voltage to test rated withstand voltages of $\pm 1550 \text{ kV}$ LI to earth superimposed to $\pm 550 \text{ kV}$ DC, whereas coupling capacitor setups would need

about ± 2100 kV generator output for the same result. This increases the size of the impulse voltage generator and the required laboratory space.

Literature describes ignition problems with spark gap test setups [13]. Especially for SI voltage tests, spark gaps are said to have an unstable triggering behavior. It has further been claimed that it is impossible to superimpose less than twice the DC voltage with spark gaps during SIMP tests with same polarity of DC and impulse voltage. And finally, literature reports arc-extinguishing effects. All these phenomena, reported for conventional LI and SI testing, were not observed for oscillating impulse voltage testing in this project [8]. Figure 6 shows the test setup for SIMP tests with OLI/OSI [8].

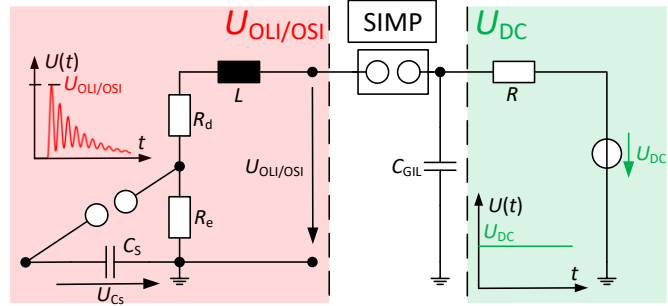


Figure 6: Superimposed (SIMP) voltage testing at 100 m GIL (C_{GIL}) with DC voltage U_{DC} and oscillating impulse voltage $U_{OLI/OSI}$ with spark gap [8]

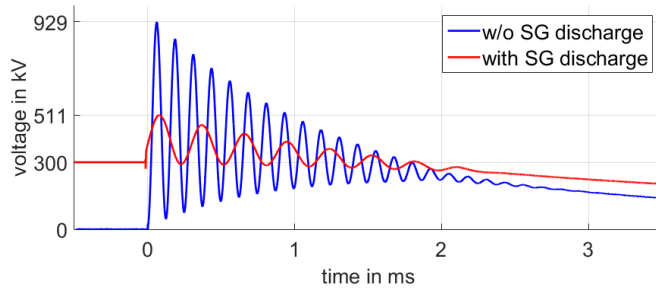


Figure 7: Voltage overshoot effect during SIMP impulse voltage testing with oscillating switching impulse voltage [8]

Therefore, the triggering of spark gaps during superimposed OLI/OSI voltage tests is working naturally without external trigger [8].

3.2. Commissioning of the dielectric test arrangement

Generally, the commissioning of a DC GIL follows the same procedure as for AC GIL installations. This section only discusses the most important steps during the commissioning process of the test arrangement under consideration. Moisture can strongly influence DC insulation systems [14]. During gas evacuation, the current source (section 3.1.1.) is also used to heat the assembly for drying the arrangement, in particular the insulators. The efficiency of the process could be controlled by monitoring the vacuum level after finishing the evacuation process [15]. If sufficiently low residual moisture is attained by the evacuation process, only a slight increase of vacuum level will be observed after finishing the process, but afterwards the level remains more or less stable. If the process was insufficient or if the tube is even untight, a distinct decrease of the vacuum level would occur. Further on, the moisture of the N_2/SF_6 gas will be controlled after the gas filling process. As much experience was collected with testing of gas-insulated systems with AC voltage, Cigré JWG D1/B3.57 recommends commissioning tests of DC GIL with AC voltage. The AC test voltage is generated by a transportable resonant unit. During the first AC voltage stress, the DC-GIL is conditioned with a defined step-by-step AC voltage increase. At the different voltage steps particles of different sizes might be activated. The particle movement can be observed by the UHF monitoring system (section 3.3.) to ensure that all potential particles are captured by the particle

traps. This process is of special importance for gas-insulated DC GIL assemblies, because free moving particles could directly trigger flashovers under DC voltage stress [6]. The final voltage step is $\hat{U}_{\text{pre-stress AC}} = 1.5 \cdot U_{\text{rdc}} = 825 \text{ kV}$ (583 kV r.m.s.) for 1 min to test the insulation system and to activate potential partial discharges. The PD measurement is performed at $\hat{U}_{\text{pd-test AC}} = 1.2 \cdot U_{\text{rdc}} = 660 \text{ kV}$ (467 kV r.m.s.). The procedure described combines the conditioning process and the experience with the AC UHF PD measurement including the well-known PRPD patterns to gather all possible information about the actual GIL insulating condition. During this procedure the AC voltage stresses will also occur at the gas-insulated voltage divider and the bushings. These components have to be designed to also withstand the AC commissioning process.

In a second step the DC GIL is subjected to oscillating impulse voltages according to IEC 60060-3. These tests shall ensure the on-site withstand voltage levels of $\pm 1240 \text{ kV OLI}$ and $\pm 940 \text{ kV OSI}$ (80 % of the rated values). In a third step the test arrangement is stressed with $\pm 660 \text{ kV DC}$ test voltage ($1.2 \cdot U_{\text{rdc}}$) for 1 h, combined with polarity reversal tests. Especially the polarity reversal test can give confidence that particles are not re-activated from the particle traps. The PD activity during DC is monitored with the UHF system. These first tests were passed successfully. After this commissioning process, further pre-tests (e.g. SIMP voltage tests) were performed according to the pre-test recommendations of the Cigré JWG D1/B3.57 (refer to clause 2).

3.3. UHF PD Monitoring

To be able to check the GIL condition during the prototype installation test and to demonstrate the performance of similar systems to later customer projects, a UHF PD monitoring system is installed at “Installation A”. Due to its regular construction principle, the GIL is comparatively predictable in its high frequency behavior compared to a GIS with a more complex interior. In terms of signal propagation, the strongest impact occurs at disc insulators due to the different permittivity compared to gaseous insulation and at changes of the line surge impedance due to structural variations of the inner and outer diameter [16]. Such steps in the surge impedance typically occur at the support insulators (Figure 1 (a)). Therefore, the number and severity of changes in surge impedance and the number of insulators are critical with regard to UHF PD signal attenuation. These phenomena strongly affect the signal transfer and the UHF measuring sensitivity.

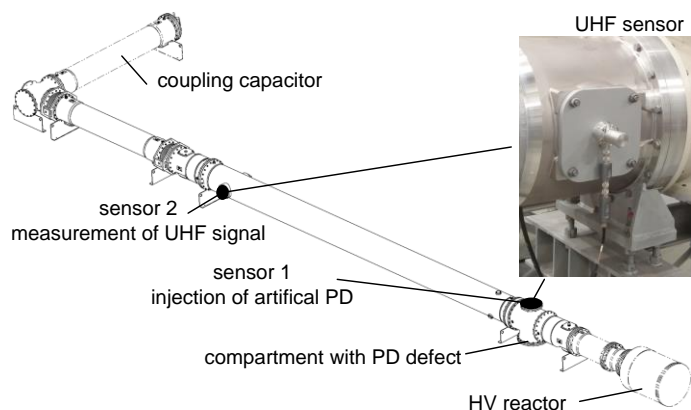


Figure 8: Test arrangement for sensitivity verification step 1

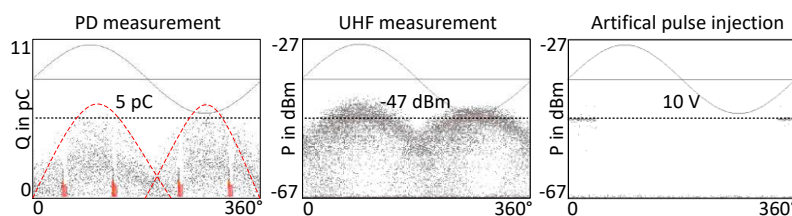


Figure 9: Test results for sensitivity verification step 1

The measuring sensitivity of the installed UHF monitoring system was tested according to the recommendations given in Cigré TB 654. As the GIL under consideration is a new design, sensitivity verification step 1 had to be performed first. It was conducted on a typical GIL structure presented in Figure 8. Two insulators and 10 m GIL were present between Sensor 1 and Sensor 2. The used surge protection and preprocessing unit at the PD sensors had a cut-off frequency from 0.3 GHz to 1.5 GHz (Figure 8). The results of the sensitivity verification step 1 are given in Figure 9. A 5 pC mobile particle PD defect measured according IEC 60270 was chosen as reference signal (Figure 9 left). This defect

corresponds to a -47 dBm UHF signal (Figure 9 middle). The equivalent UHF signal for 5 pC moving particle is generated by 10 V artificial impulses (Figure 9 right). The injection voltage for sensitivity verification test step 2 is therefore 10 V to prove that a 5 pC mobile particle PD defect can be detected between two adjacent sensors.

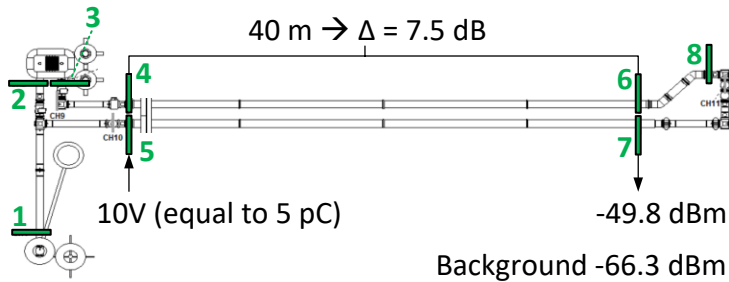


Figure 10: Position of UHF sensors (green) and sensitivity verification step 2 results

The sensitivity verification step 2 was carried out within the frame of the commissioning tests of the test arrangement. The positions of the UHF sensors are illustrated in Figure 10. The GIL section is fitted with the sensors nos. 4... 8. The other sensors nos. 1... 3 are installed in the connecting modules to the current and voltage source. The artificial

pulse of 10 V was injected in one sensor and the corresponding PD signal recorded at the adjacent sensors. The signal at the adjacent sensors was at minimum -49.8 dBm. The lowest values were measured at the elbow modules. The sensitivity verification demonstrates that PD defects at “Installation A” distinctly smaller than 5 pC can be detected in between of two adjacent sensors. Figure 10 shows the attenuation of the section between sensor 4 and 6, 40 m in length, which amounts to about 7.5 dB in average. It can be concluded that a sensor distance of some hundred meters would still be sufficient to detect 5 pC defects at the new DC GIL design.

As no phase correlation exists at DC voltage, pulse amplitude and pulse sequence have to be evaluated for the characterization of PD defects. Thus, the partial discharge monitoring device has to provide time stamped events of the occurring partial discharge. The used system allows the continuous and parallel acquisition of several hundred sensors of time-stamped partial discharge signals [16]. Pulses above threshold values are thereby visible and countable, which allows a first PD analysis of the arrangement. Another approach is the statistical analysis of the PD pulse sequence (PSA). A common option is the NoDi*-diagram in which the amplitude or time difference of successive pulses i and $i+1$ is determined [19]. A similar approach reports different evaluation methods for this data in [17]. Pre-tests with PSA methods were performed and shall be further investigated for the dielectric test assembly during the DC long-term stress.

4. Soil mechanics test arrangement (“Installation B”)

In 2010 the first 1 km directly buried AC GIL with temporarily flowable backfill (TFB) was installed in the area of Frankfurt airport (“Kelsterbach”) [1], [15]. This pilot installation was designed in a conservative way regarding the thermal and mechanical properties of the backfill. E.g. the current rating could be increased from 2700 A AC to 3150 A AC, since measured temperatures during operation remained far below the technical limits [18]. DC GIL solutions would be more competitive to other systems by utilizing the benefits of higher current ratings and/or lower heating. Detailed thermal and mechanical measurements are thus required to further optimize the GIL rating calculations as well as the mechanical dimensioning of future directly buried GIL installations. “Installation B” closes this gap and collects more data about mechanical soil-structure-interaction (“SSI”; e.g. displacements, strains, stresses, forces) and resulting temperatures when a DC current of 5000 A DC is fed into the directly buried DC GIL (“HL”). Since the mechanical SSI is independent of high voltage stress, the test is carried out with current only. The gas compartments are filled with nitrogen. This represents a more critical thermal arrangement as with the N_2/SF_6 mixture, but allows easier gas handling. Differences of the measured temperature distribution when changing the gas parameters can easily be simulated. “Installation B” is periodically stressed with high load (“HL”) and current pauses to trigger GIL-soil displacements and to investigate the temperature rise.

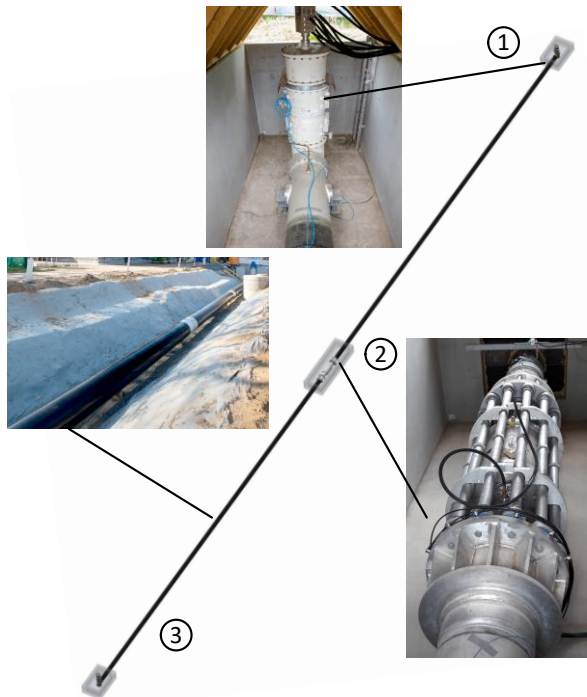


Figure 11: Soil mechanics test arrangement (130 m)

The first mechanical load cycles were 30 days “HL” cycle and 30 days pause so far (60 days in total). The results presented in the following were gained after two mechanical load cycles.

“Installation B” is shown in Figure 11. The directly buried DC GIL with a length of about 130 m is installed in a trench at a depth (conductor axis) of 1.35 m. The space between TFB and ground surface (height 0.9 m) is covered with the excavated soil, which allows simple agricultural use at practical installations. There are two concrete shafts at both ends of the GIL (1 and 3) and one in the center (2). At both ends (1 and 3) the GIL consists of an elbow module and a short vertical compartment, which is connected to the busbar of the power source. The busbar connection, as well as the steel structure is designed to allow a free movement of the GIL in axial direction, which is essential for the displacement measurement. The center shaft (2) is used for mechanical measurements: The contact forces from “SSI” restraining the

movement of the GIL enclosure tube in an area around the center of the installation result in compressive stresses in the enclosure tube, which can lead to buckling of the GIL enclosure. Load cells are installed to measure the axial forces inside the GIL enclosure tube by redirecting the axial forces. An axial compensator is used to make the enclosure tube flexible enough to not transfer axial forces. Brackets are welded to the enclosure tube on each side of the compensator. Steel beams in series with load cells connect the brackets (2) to measure the forces inside the enclosure tube.

4.1 Soil-Structure-Interaction

The GIL can be mechanically fixed in the soil material by just relying on the natural contact forces between enclosure tube and backfill. To investigate this mechanism, the movement and deformation of the enclosure tube especially in the sliding area towards both ends and the force resulting from restrained thermal expansion in the middle of the test setup are measured. Furthermore, the movement of the GIL enclosure tube in relation to the shaft wall is measured to check if there is a naturally fixed area where the contact forces to the backfill are higher than the forces of restrained thermal expansion in the enclosure tube.



Figure 12: TFB Consistency test on site

The DC GIL is embedded in a temporarily flowable backfill (TFB). The TFB itself is shown in Figure 12. Major advantages of this material are re-use of the excavated material, high contact forces that restrain the GIL displacement and high and stable thermal conductivity to optimize heat transfer. The soil mixture is adapted and optimized to the excavated sand. The TFB for “Installation B” consists of about 70 % excavated soil, 25 % water and 5 % bentonite and cement. Figure 12 shows the used mixture during the consistency test. The diameter of the flowed material in Figure 12 is a measure of the flowability and its later self-compacting characteristics in the trench [15]. Moisture contents and pore water pressures/ tensions are monitored in the TFB close to the GIL and in the adjacent soil. In the

monitoring period June to December 2019, moisture contents and pore water tensions in the TFB are approximately constant in a range of 35 to 45% and < 150 hPa, respectively, not significantly affected by heating. Consequently, TFB provides a stable thermal conductivity in the range of $1.8 \text{ W}/(\text{m}\cdot\text{K})$.

The contact forces of the TFB restrain the movement of the enclosure tube due to thermal expansion. After the two cycles displacements less than 5 mm for 65 m GIL have been measured at the free-end in shaft 1 (Figure 11). A completely free and not embedded aluminum bar would experience a displacement of ≈ 26 mm for $\Delta T = 20$ K (the temperature rise according to section 4.2). The measured axial forces correlate to the measured temperature differences ΔT at the enclosure tube and remain in the predicted ranges. So, it can be concluded that the TFB-embedding effectively reduces the expansion and displacements of the GIL enclosure tube. The results clearly show that neither suspected gaps between backfill and enclosure tube, nor lifting or buckling of the enclosure tube due to thermal forces will occur in practice. Further high load cycles to evaluate the technical limits of the systems will be carried out over the next months. The measuring systems, as well as the graphs for the “SSI” will be presented and discussed in further publications.

4.2 Soil temperature distribution

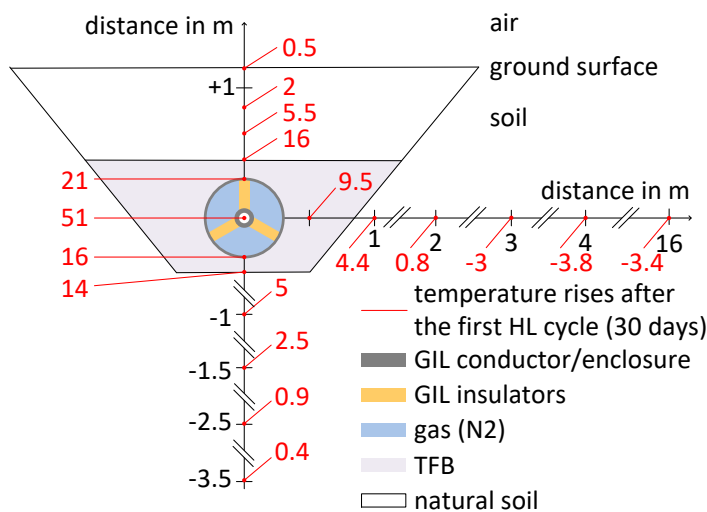


Figure 13: TFB-embedded GIL cross section: monitored maximum temperature rises after the first HL cycle

The temperature distribution of the directly buried assembly is of high importance for the thermo-electric design of the insulation system. These data are also useful to adjust the temperature rise at “Installation A”, as well as to optimize the soil mechanical design in general. Figure 13 shows the principle temperature distribution of “Installation B”. The maximum temperature rises at each cross-section point for the first “HL” cycle from October 2019 to November 2019 are given in Figure 13. The temperature rises are defined as the differences of temperatures before and after four weeks of “HL” current stress. The average ambient temperature before the test was in the range of 20 °C. The temperature rise of the GIL conductor is reproducible in both cycles and remains < 60 K. The measured temperature rise at the enclosure tube reaches a maximum of $\Delta T = 21$ K on its top. The maximum temperature gradient at the insulators is thereby 30 K. The ambient temperature decreased during the first “HL” cycle because of changes in the weather. The temperature rise of the sensors with 3 m, 4 m and 16 m distance is therefore negative. These first results generally confirm the comparatively low temperature rises around a GIL, even in this worst-case scenario test with permanent 5000 A DC energization and thermally unfavorable 100 % N_2 gas insulation of this test installation. A significantly lower thermal impact during service with lower current ratings and/or partial load of the DC GIL transmission system is expected. The temperature rises after four weeks “HL” cycles were not yet stationary. In further “HL” cycles the temperature rises will be further investigated. The results will also be presented and discussed in further publications.

5. Conclusion and further steps

The report presents a new DC GIL prototype for HVDC transmission above-ground, tunnel or directly buried installation. The insulators, as well as the particle traps were optimized to be able to

withstand all DC and transient voltage stresses. Although laboratory tests were performed to investigate the performance of the new design, these tests do not replace service experience after on-site installation conditions with this new type of equipment. To prove the long-term performance and to collect more service experience at practical conditions, the DC GIL prototype is tested in a one year “prototype installation test” according to proposals of Cigré JWG D1/B3.57. The test is carried out on a 100 m DC GIL, mostly installed outdoor. The test consists of high load and zero load cycles at a DC test voltage of 1.2 U_r. High load is generated by a novel DC current injection source. DC current provides a couple of advantages over AC current loading. It further corresponds to the later operation in the grid. Laboratory experience with this novel generator concept has shown good performance. After each cycle superimposed voltage tests are performed. These tests are carried out with oscillating impulse voltage. A spark gap is used as coupling element. Laboratory experience with this new approach has shown good performance of the overall setting. The GIL is monitored by an UHF monitoring system during the long-term test. The sensitivity verification according to Cigré TB 654 on the new design shows a sensitivity of the monitoring system of the test arrangement sufficient for detection of the common PD defects. The commissioning process mainly follows the same procedure as for AC GIL and has been extended to cover some special DC phenomena. First tests were successfully passed.

The soil-structure interaction as well as the temperature rises are investigated at a second, directly buried 130 m long DC GIL. It is embedded in temporarily flowable backfill, which ensures high and stable heat conductivity and contact forces, thus restraining the GIL movement. The test is performed at DC current stress only (without high voltage applied). First high load cycles have shown temperature rises far below the technical GIL limits. The temperature rise of the natural soil due to GIL heating is comparatively low in comparison to other effects like sun radiation. The temporarily flowable backfill shows a good thermal and mechanical performance so far.

Acknowledgments

The authors gratefully acknowledge the substantial support of this work by the IWB-EFRE-Program by the State of Hessen (Funding Code 20002558) and the German Federal Ministry of Economics and Technology (Funding Code 03ET7546).



Supported by:



on the basis of a decision by the German Bundestag

BIBLIOGRAPHY

- [1] H. Koch: "Gas-Insulated Transmission Lines", ISBN 978-0-470-66533-6, IEEE Press / John Wiley & Sons, 2012.
- [2] Siemens AG: "www.siemens.com/GIL" as consulted online on 29th December 2019
- [3] J. Alter, S. Poehler, Ch. Lueger, C. Neumann: „Experience at commissioning of the 380-kV-GIL in Munich-Langwied“ (in German language) In: Conference of GIS Userforum, Darmstadt, Germany, Oct. 14, 2014
- [4] T. Magier, M. Tenzer, H. Koch: "Direct Current Gas-Insulated Transmission Lines", IEEE Transactions on Power Delivery, VOL. 33, NO. 1, Pp. 440-446, ISSN 0885-8977, February 2018.
- [5] A. Diessner and J. G. Trump, "Free conducting particles in a coaxial compressed-gas-insulated system," IEEE Trans. Power App. Syst., vol. PAS-89, no. 8, pp. 1970–1978, Nov./Dec. 1970.
- [6] T. Berg, H. Koch, K. Juhre: "Free Moving Particles in Gas-Insulated Lines Under DC Conditions – Basic Properties, Specific Effects and Countermeasures" In: 21st International Symposium on High Voltage Engineering (ISH), Budapest, Hungary, 26-30 August 2019
- [7] C. Neumann, M. Hallas, M. Tenzer, M. Felk, U. Riechert: "Some thoughts regarding prototype installation tests of gas-insulated HVDC systems", CIGRÉ A3, B4 & D1 International Colloquium, Winnipeg, Canada, September 30 – October 6, 2017
- [8] M. Hallas, C. Dorsch, V. Hinrichsen: "Superimposed Voltage Testing of HVDC Equipment with Oscillating Impulse Voltage" In: IEEE International Conference on High Voltage Engineering and Application (ICHVE), Athens, Greece, 10. - 13. September 2018
- [9] M. Hering, H. Koch, K. Juhre: "Direct Current High-Voltage Gas-Insulated Switchgear up to ±550 kV", CIGRE-IEC 2019 Conference on EHV and UHV (AC & DC), Hakodate, Hokkaido, Japan, April 23-26, 2019
- [10] M. Hallas, V. Hinrichsen: "General overview of AC and DC current injection on high voltage potential for HVDC long-term tests" In: Cigré-IEC 2019 Conference on EHV and UHV (AC & DC), Hakodate, Japan, 23-26 April 2019
- [11] H. Appelo, M. Groenenboom, J. Lisser: "The zero-flux DC current transformer – a high precision bipolar wide-band measuring device". IEEE Trans. Nuclear Science, vol. 24, no. 3, pp. 1810-1811, 1977.
- [12] M. Hallas, T. Wietoska, V. Hinrichsen: "Construction of a DC Current Injection Generator for HVDC Long-term Tests up to 5000 A DC at 660 kV DC Potential" In: 21st International Symposium on High Voltage Engineering (ISH), Budapest, Hungary, 26-30 August 2019
- [13] A. Voß, M. Gamlin: "Superimposed Impulse Voltage testing on Extruded DC Cables Ac-cording to IEC CDV 62895" In: 20. International Symposium on High Voltage Engineering (ISH), Buenos Aires, Argentina, August 28 – September 01, 2017
- [14] K. Juhre, M. Hering: "Influence of extreme temperature conditions on the gas-solid insulating system under DC voltage stress", CIGRÉ Winnipeg 2017 Colloquium, paper D1-163, Winnipeg, Canada, September 30 – October 6, 2017
- [15] C. Neumann, S. Poehler: "First Pilot Installation of a 380 kV directly buried Gas Insulated Line (GIL)" In: Jicable Conference, Versailles – France, Paper B5.6., 19 - 23 June 2011 -
- [16] D. Gross: "Partial discharge signal transmission of distributed power engineering equipment" In: Intl. Conference on Diagnostics in El. Engineering (Diagnostics), Pilsen, Czech Republic, Sept. 4-7, 2018
- [17] P. Wenger, M. Beltle, S. Tenbohlen, U. Riechert: "PD-Characteristic of Free Moving Particles in HVDC-GIS using UHF Measuring Technique and High-Speed Imaging" In: VDE-Hochspannungstechnik, Berlin Germany, 10.11.2018
- [18] S. Poehler, P. Rudenko: "Directly buried gas-insulated transmission lines (GIL)" In: PES T&D, USA, Orlando, FL, pp. 1-5, 7-10 May 2012
- [19] A. Pirker, U. Schichler, "Partial Discharge Measurement at DC Voltage - Evaluation and Characterization by NoDi* Pattern", In: IEEE Transactions on Dielectrics and Electrical Insulation, Vol. 25, No. 3, pp. 883 891, 2018